

# Small and Large Scale Granular Statics

Chay Goldenberg<sup>1</sup> and Isaac Goldhirsch<sup>2</sup>

**Abstract** Recent experimental results on the static or quasistatic response of granular materials have been interpreted to suggest the inapplicability of the traditional engineering approaches, which are based on elasto-plastic models (which are elliptic in nature). Propagating (hyperbolic) or diffusive (parabolic) models have been proposed to replace the ‘old’ models. Since several recent experiments were performed on small systems, one should not really be surprised that (continuum) elasticity, a macroscopic theory, is not directly applicable, and should be replaced by a grain-scale (“microscopic”) description. Such a description concerns the interparticle forces, while a macroscopic description is given in terms of the stress field. These descriptions are related, but not equivalent, and the distinction is important in interpreting the experimental results. There are indications that at least some large scale properties of granular assemblies can be described by elasticity, although not necessarily its isotropic version. The purely repulsive interparticle forces (in non-cohesive materials) may lead to modifications of the contact network upon the application of external forces, which may strongly affect the anisotropy of the system. This effect is expected to be small (in non-isostatic systems) for small applied forces and for pre-stressed systems (in particular for disordered systems). Otherwise, it may be accounted for using a nonlinear, incrementally elastic model, with stress-history dependent elastic moduli. Although many features of the experiments may be reproduced using models of frictionless particles, results demonstrating the importance of accounting for friction are presented.

*Received: August 15, 2018*

Chay Goldenberg<sup>1</sup> and Isaac Goldhirsch<sup>2</sup>

<sup>1</sup>School of Physics and Astronomy  
Tel-Aviv University  
Ramat-Aviv, Tel-Aviv 69978, Israel  
e-mail: [chayg@post.tau.ac.il](mailto:chayg@post.tau.ac.il)

<sup>2</sup>Department of Fluid Mechanics and Heat Transfer  
Faculty of Engineering  
Tel-Aviv University  
Ramat-Aviv, Tel-Aviv 69978, Israel  
e-mail: [isaac@eng.tau.ac.il](mailto:isaac@eng.tau.ac.il)

We appreciate helpful interactions with R. P. Behringer, J. Geng, E. Clément, D. Serero, H. Jaeger, T. A. Witten, N. Mueggenburg and J.-N. Roux. Support from the U.S.-Israel Binational Science Foundation (BSF), INTAS and the Israel Science Foundation (ISF) is gratefully acknowledged.

**Key words.** Granular response – elasticity – coarse-graining

## 1 Introduction

The modeling of granular materials has been a subject of ongoing research in the engineering community (see e.g., [1]). In recent years, this subject has found renewed interest among physicists [2–5] (having been studied in the distant past by great physicists such as Coulomb, Faraday, Reynolds and others).

The behavior of “granular gases”, which are obtained by e.g., sufficiently strong shaking or shearing (so that the material behavior is dominated by interparticle collisions), has been quite successfully modeled using approaches based on extensions of the kinetic theory of gases [6]. However, the behavior of dense granular matter, which is dominated by prolonged interparticle contact, has proven more difficult for modeling. For the description of the quasi-static behavior, elasto-plastic models are commonly used by engineers [7, 8].

This paper is concerned with the static behavior of granular systems. In elasto-plastic models, one often uses (linear) elasticity below yield (although parts of a static system are sometime assumed to be at incipient yield [8]). However, in recent years a very different class of models has been proposed for describing the statics of granular materials, based on the notion of “force propagation”, suggested by the observation of force chains in experiments on granular materials [9], as well as simulations [10, 11]. These models (see e.g., [12–15]) typically yield hyperbolic partial differential equations for the stress field, in contrast with the elliptic, non-propagating nature of the classical equations of static elasticity. It has been claimed that the hyperbolic description tends to an elastic-like one at large scales [16–18] (however, the physical interpretation of the macroscopic fields in this case is not clear).

Recently, the response of granular slabs resting on a horizontal floor to a ‘point force’ applied at the center of the top of the system has been studied experimentally [19–25]. In [19, 22, 23], the intergrain force distribution has been measured in two-dimensional (2D) systems as a function of vertical and horizontal distance from the point of application of the force. In [25], the particle displacements for similar 2D systems have been measured. In [20, 21, 24], the vertical force acting on the floor has been measured in three-dimensional (3D) systems. Prominent force chains

have been observed in ordered 2D systems; these force chains fade out with increasing disorder. For pentagonal particles in 2D arrangements the measured force distribution is single peaked and the width of the peak is linearly related to the vertical distance, in conformity with elasticity. The results for cuboidal particles obtained in [19] appear to suggest a parabolic behavior, consistent with a diffusive model, although the systems studied were quite small. In [25], the width of the measured distribution of displacements, as a function of the vertical distance from the particle which is directly displaced, follows a square root dependence (as expected from a diffusive model) for small distances of a few particle diameters, crossing over to a linear dependence at larger distances (consistent with an elastic description). Ordered 3D packings exhibit multiple force peaks for shallow systems [24] and less structure for deeper ones. Somewhat larger (in terms of number of particles), disordered 3D systems [20, 21] exhibit a single peak in the force distribution measured at the floor, whose width is proportional to the depth of the system.

The experimental evidence appears to be contradictory: different experiments seem to support fundamentally different descriptions of the response of granular materials (in the case of 2D systems, it has been suggested that there may be a crossover from a hyperbolic to an elliptic behavior with increasing disorder [22]). The thesis presented in this paper is that these seemingly contradictory experimental results (and theoretical explanations) are not necessarily at odds with each other. This thesis is based on the observation that most of the studies (perhaps all) rejecting the elliptic description have been devoted to small systems, of the size of a few dozen of particle diameters at most, whereas many engineering studies consider rather large granular systems. Since elasticity and other *macroscopic* descriptions are not valid on small scales, at which local anisotropies and randomness play a major role, one should not be surprised that such descriptions fail on small scales. Indeed, simulations [26, 27] reveal the existence of a crossover from microscopic to macroscopic behavior of granular assemblies (as well as other systems [28]) as a function of system size or resolution. We argue that such a crossover is observed in some of the experiments mentioned above. Strictly isostatic systems [29] have been shown to be described by hyperbolic stress equations [15, 30], and numerical simulations suggest that systems of frictionless spherical particles approach isostaticity in the limit of infinite rigidity [31]). However, we argue that since real granular systems have finite rigidity and usually experience frictional interactions, they cannot be generically isostatic (the same presumably holds even for frictionless non-spherical grains). The isostatic limit is a singular case, whose physical consequences for *real* systems are at best unclear. Therefore the controversy surrounding the correct description of granular statics is mostly a question concerning the behavior of small granular systems. The latter require a grain-scale (“microscopic”) description, rather than a macroscopic one.

A second point stressed below is the distinction between *force* and *stress*. Whereas interparticle forces can exhibit force chains which look like they contradict elasticity, the latter does not describe the nature of the forces

but rather that of the stress field. The stress field involves an averaging over the forces (whose result is resolution dependent) and leads to less pronounced structure than the underlying force field. The small scale structure of the interparticle forces cannot be taken to consist an argument against an elliptic description or in favor of it, since it relates to small scales and it does not deal with the objects with which elasticity or plasticity are concerned. The large scale response of granular packing is shown to be consistent with a (possibly anisotropic) elastic description. The fact that in non-cohesive granular materials there is no significant attraction among the particles may lead to modifications of the contact network, which may strongly affect the anisotropy of the system. This effect is expected to be small for small applied forces (for non-isostatic systems) and for pre-stressed systems, in particular for disordered systems. Otherwise, it may be accounted for using a nonlinear, incrementally elastic model, with stress-history dependent elastic moduli.

The third point made in this paper is that while models employing frictionless particles can reproduce some properties of granular packings, friction can be of utmost importance for the description of granular matter (a rather intuitive fact). Results demonstrating the importance of accounting for frictional interactions are presented in Sec. 5.

## 2 The microscopic picture: forces

In attempting to describe granular materials in terms of continuum mechanics, by analogy to “regular”, atomic materials, one usually considers the “microscopic” scale to be that of the individual particles (whose internal dynamics should be well described by continuum mechanics).

One of the simplest granular systems is a collection of frictionless spherical particles. A typical microscopic (particle scale) description of such a system is given by the particle’s radii,  $\{R_i\}$ , their masses,  $\{m_i\}$ , center of mass positions,  $\{\mathbf{r}_i(t)\}$ , and velocities,  $\{\mathbf{v}_i(t)\}$ , at time  $t$ . It is typically assumed (e.g., in the context of simulations of granular materials [10, 32, 33]) that the particles are quite rigid, so that the interaction between two particles (in the frictionless case) depends only on their respective distance, or, more conveniently, on their imaginary overlap  $\xi_{ij}(t) \equiv R_i + R_j - |\mathbf{r}_{ij}(t)|$ , where  $\mathbf{r}_{ij}(t) \equiv \mathbf{r}_i(t) - \mathbf{r}_j(t)$ . The contact interactions are usually modeled by treating the particles as macroscopic objects, described by the equations of continuum mechanics (see e.g., [34, 35]). For two frictionless elastic spheres, a classical result by Hertz (see e.g., [36]) is that the force is proportional to  $\xi^{3/2}$ , while for cylinders, it is linear in the overlap. For noncohesive particles, only repulsive forces are possible. Even for frictionless particles, internal dissipation as in e.g., viscoelastic particles, gives rise to a dependence of the force on the relative velocity  $\dot{\xi}$  as well (for some examples of force schemes commonly used in simulations, see e.g., [37–39]).

The interparticle forces for a given configuration of such particles subject to given boundary conditions (e.g., specified displacements of the particles on the boundary, or forces applied to them) and body forces such as gravity can be determined, for a static system, using the equations

of equilibrium (Newton’s laws) and the force-displacement relation. We reiterate that when full force laws for particle interactions are known or modeled, the statics and dynamics of the system are fully determined (they may be history-dependent for history-dependent force laws, as commonly used for frictional interactions).

In the case of frictionless isostatic systems (in which the mean coordination number is *exactly*  $z = 2d$ , where  $d$  is the dimension of the system) the forces can be determined from the equations of equilibrium alone (and are therefore independent of the force-displacement law; however, the particle *displacements* certainly depend on this law). It has been suggested [40, 41] that frictionless granular systems become isostatic in the limit of infinite rigidity (giving rise to a macroscopic behavior which is very different from elasticity), and this appears to be borne out by numerical simulations [31, 42]. However, the relevance of this limit to real materials is questionable, since real materials cannot be infinitely rigid. Any additional contacts created if the rigidity is allowed to be finite will render the system hyperstatic (so that there is a “phase transition” to an isostatic behavior *only* at infinite rigidity [40]). The rigidity should of course be compared to the confining forces or body forces (in a system under gravity and confined by walls, the confining force is related to gravity). If the confining forces are very small, the system would indeed be expected to be close to marginal stability. As mentioned above, the static indeterminacy associated with hyperstatic systems simply means that the equations of equilibrium are insufficient for determining the forces, so that additional equations (e.g., force-displacement laws) are required. Static indeterminacy *does not* mean that there’s no unique solution for the forces in a *real* system. A similar situation occurs on the macroscopic, continuum level (see e.g., [8]). The rigid limit can be approached in many different ways (e.g., the stiffness of each interparticle contact may be different), and, even if assuming that the same (isostatic) contact network is obtained for different distribution of the interparticle stiffness, yielding the same interparticle forces, the particle displacements will certainly be different, hence the rigid limit is not unique, at least in this sense.

In several experiments, photoelastic particles were used in order to measure the stress in granular systems [9, 19, 22, 23, 43]. These measurements probe the *intraparticle* stress, i.e., the stress *inside* each particle. Following the above, these should be interpreted as measurements of microscopic fields (the macroscopic description of granular systems regards the particles as microscopic, and does not resolve any details below the particle scale). The microscopic fields corresponding to these measurements are the interparticle forces, which can be deduced from these internal stress measurements (as described in [23]). As mentioned, these forces should be distinguished from the “macroscopic” stress field in the system.

The distribution of force magnitudes in a static granular packings is a microscopic quantity which has been extensively studied in experiments [44, 45] and simulations [46]. An exponential behavior of the distribution at large forces appears to be quite universal in experiments on granular systems, independent of the degree

of disorder [45], the friction coefficient [45], or the rigidity of the particles [47], and has also been observed in simulations of granular systems with different models for the interparticle forces (e.g., [48, 49]). The universality of the force distribution appears to extend to other systems such as foams, glasses, colloids etc. (see [50] and references therein). The exponential tail of the distribution is reproduced in simple models such as the (parabolic) q-model [51, 52]. The distribution for smaller forces appears to be less universal, and it has been suggested that the appearance of a peak in the force distribution near the mean force may signal the onset of jamming or a glass transition [53].

Interestingly, a qualitatively similar force distribution is obtained in purely harmonic networks: Fig. 1 shows the force distribution obtained for an ensemble of random networks of linear springs constructed as follows. Points are placed on a 2D triangular lattice with spacing  $d$  (with square-shaped boundaries), and then their  $x$  and  $y$  coordinates are randomly displaced by  $\pm 0.04d$ . Points whose distance is less than  $1.02d$  are connected by linear springs (whose equilibrium length is equal to this distance) with equal spring constants (this results in an average dilution of about 12% of the springs compared to the perfect lattice). A uniform isotropic compression of 1% is applied to the boundary particles, and the interparticle forces are calculated. The force distribution presented in Fig. 1 is obtained from an average over the force histograms of 100 systems of 1085 particles. The force was normalized by the mean force in the ensemble (a similar distribution is obtained for a normalization by the mean force for each system; the variation in mean force among different systems is relatively small, which may indicate that the system is far from ‘jamming’ [53]). The tail of the logarithm of the distribution is fit quite well with a line of slope  $-3.8$ , similar to the slope obtained in experiments on highly compressed disordered packings of soft rubber spheres [47] (similar distributions were obtained for a scalar harmonic network of unequal springs in [48]). For the case of networks with no force dilution (the same connectivity as in the perfect lattice), the force distribution is Gaussian with a half-width of a few percent of the mean, i.e., a much narrower distribution). These results indicate that a random connectivity should be consequential for the force distribution, which may be the reason that even for highly compressed disordered spheres (whose contact network is still disordered), the distribution is qualitatively similar to that observed in less compressed systems [47]. A similar effect has been observed in simulations of granular systems under different applied pressures [48].

The forces in one of the realizations of the ensemble are shown in Fig. 2. Force chains are clearly observed (note that there are very few tensional forces, so that they do not significantly affect the force distribution in this case). Similar force chains have been observed in a polydisperse Lenard-Jones system [28] (incidentally, the concept of a force chain is not well-defined: in the case of a homogeneous strain applied to a uniform lattice, the forces are equal, so that it is reasonable to define the force chains to contain forces whose magnitude is larger than a uniform cutoff, e.g., the mean force, as used in Fig. 2; However,

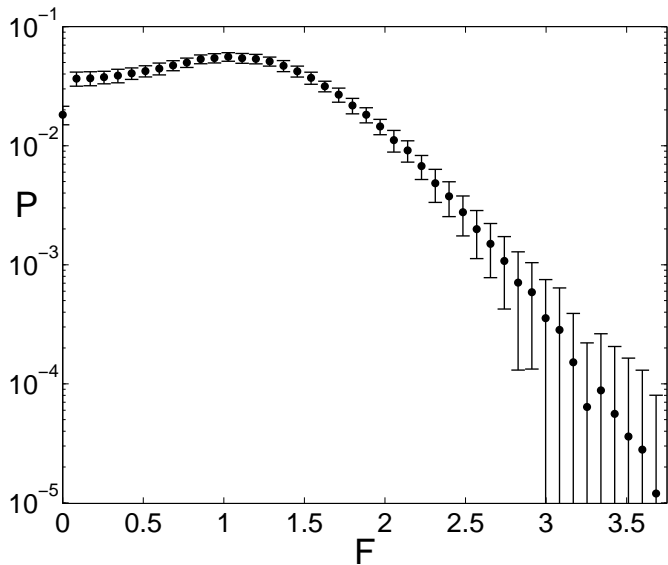


**Fig. 1.** The distribution of force magnitudes in bond-diluted distorted triangular networks of linear springs (see text).

for a non-uniformly strained system, e.g., systems subject to gravity, in which the mean force increases with depth, such a global cutoff makes little sense). The results shown in Fig. 2 indicate that force chains are not specific to granular systems. Force chains are *microscopic* features of microscopically disordered systems (or even inhomogeneously strained ordered systems, as described below), and their presence does not necessarily indicate any macroscopic inhomogeneity, or inconsistency with a macroscopic elliptic, or elastic, description. It is quite certain that if one could observe the individual interparticle forces in atomic systems (which may not be quite well defined, since a quantum description is appropriate for such systems), one would also observe force chains.

It is important to note that a significant portion of the stress (even in a homogeneously strained system) is carried by forces which do not belong to the force chains. An example is provided by a system of frictionless polydisperse disks (with radii uniformly distributed within 10% of the maximum radius) which is confined by side walls and a floor, with a uniform force applied to the particles of the “top” layer (without gravity). The interparticle forces are taken to be linear in the overlaps. Fig. 3 shows the forces in the system. Fig. 4 shows the fraction of the applied vertical force carried by the forces whose magnitude is greater than the mean (i.e., those belonging to force chains, using the definition mentioned above), compared to that carried by all the forces (which is of course equal to 1), for forces in horizontal “slices” of the system, as a function of the vertical coordinate,  $z$ . As seen in Fig. 4, only about 80% of the applied force is carried by the force chains. Furthermore, the force carried by the chains fluctuates with depth, so that the forces in the chains do not obey the conditions of force equilibrium. It is therefore questionable whether a model which describes the stress exclusively in terms of the force chains is justifiable.

The (near-)universality of the force distribution, in particular the fact that it is observed in simulations of ran-

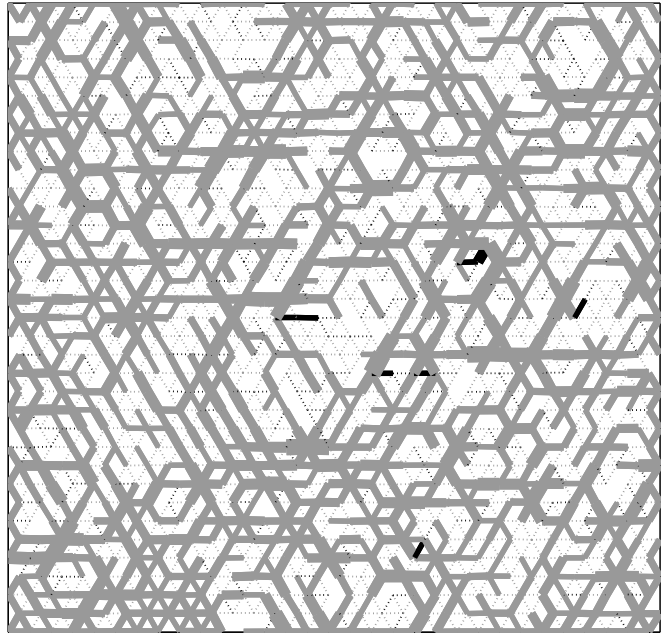


**Fig. 2.** The forces in a bond-diluted distorted triangular network of linear springs. Forces with magnitude larger than the mean are indicated by solid lines whose width is proportional to the force magnitude; smaller forces are indicated by thin dotted lines. Compressive forces are indicated by gray lines; tensile forces by black lines.

dom systems with harmonic interactions, does not make possible the differentiation between different models on the basis of the force distribution (in particular, the observation of such a distribution does not preclude an elliptic description). The same statement applies to the observation of force chains. A more sensitive and direct test should be rendered by the response of a granular system to inhomogeneous external forcing, such as that provided by localized forces. The latter seem to be consistent with elasticity, as described below.

### 3 Macroscopic fields and continuum equations in terms of microscopic quantities

Continuum descriptions of materials are often based on phenomenological arguments (usually motivated by experimental findings), rather than on derivations from the underlying microscopic dynamics. A unique feature of granular materials is that due to the typically large sizes of the constituents, it is relatively easy to access the “microscopic” scales experimentally. On the other hand, in most practical applications, the number of particles is such that a detailed particle-level description becomes intractable, and a continuum description is required. The fact that experiments on granular systems can yield both microscopic information and macroscopic information (possibly even in the same experiment) is useful to the elucidation of the connection between these two descriptions.

In order to obtain a macroscopic description of a system in terms of the microscopic fields, we employ a spatial coarse-graining approach [27, 54]. We stress that the only

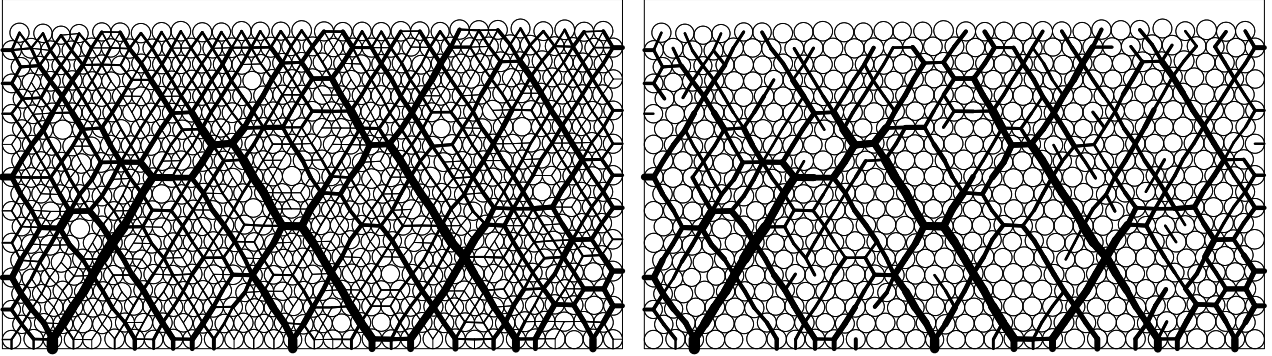


**Fig. 3.** The forces in a system of polydisperse frictionless disks with a uniform force applied to the top layer (no gravity). Line widths are proportional to the force magnitudes. Left: all forces, right: only the forces whose magnitude is larger than the mean.

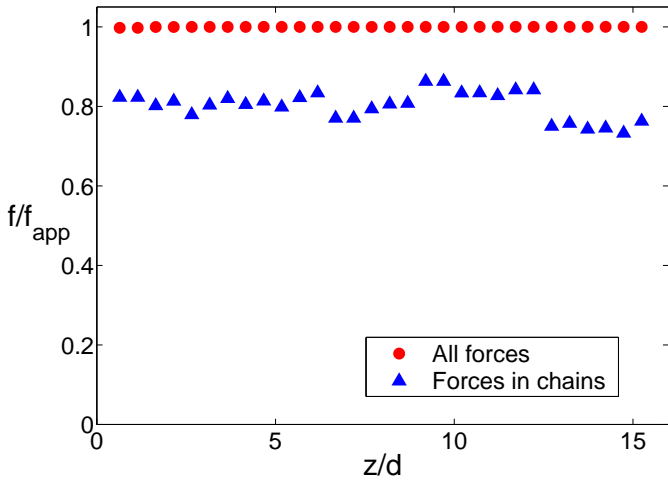


**Fig. 4.** The fraction of the applied vertical force carried by all the forces and by the forces whose magnitude is larger than the mean (i.e., those belonging to force chains), as a function of the vertical coordinate,  $z$ , scaled by the mean particle diameter,  $d$ , for the system shown in Fig. 3.

averaging considered here is spatial (the approach can be extended to include temporal coarse-graining as well [54], but here we consider static configurations). Since static granular packings are typically found in metastable states, far from equilibrium, and thermal energy scales are negligible, such systems do not explore any phase space so that it is hard to justify the kind of ensemble average commonly used in statistical mechanics. An average over configurations (i.e., average over different disordered systems which are presumed to be prepared in the same way) is commonly performed when analyzing experimental data, due to the large fluctuations obtained in many experiments. However it is not clear a-priori if self-averaging occurs, i.e., that at least for large enough scales the macroscopic behavior of a single “typical” realization is the same as that of the average behavior over many realizations. Self-averaging may be valid for some quantities and not for others. Therefore we choose not to assume a-priori that any ensemble averaging is justified; instead we relate the macroscopic and microscopic fields in a way that is relevant for single realizations.

Following [54], define the coarse-grained (CG) mass density  $\rho(\mathbf{r}, t)$  and momentum density  $\mathbf{p}(\mathbf{r}, t)$  at position  $\mathbf{r}$  and time  $t$  as

$$\rho(\mathbf{r}, t) \equiv \sum_i m_i \phi[\mathbf{r} - \mathbf{r}_i(t)], \quad (1)$$

$$\mathbf{p}(\mathbf{r}, t) \equiv \sum_i m_i \mathbf{v}_i(t) \phi[\mathbf{r} - \mathbf{r}_i(t)], \quad (2)$$

where  $\phi(\mathbf{R})$  is a non-negative coarse-graining function (with a single maximum at  $\mathbf{R} = 0$ ) of width  $w$ , the coarse-graining scale, and  $\int \phi(\mathbf{R}) d\mathbf{R} = 1$ .

Upon taking the time derivative of the macroscopic fields  $\rho$  and  $\mathbf{p}$ , performing straightforward algebraic manipulations [54] and using Newton’s laws, one obtains the equation of continuity and the momentum conservation equation, respectively:

$$\begin{aligned} \dot{\rho} &= -\text{div}(\rho \mathbf{V}) \\ \dot{p}_\alpha &= -\sum_\beta \frac{\partial}{\partial r_\beta} [\rho V_\alpha V_\beta - \sigma_{\alpha\beta}], \end{aligned} \quad (3)$$

where the velocity field is defined by  $\mathbf{V} \equiv \mathbf{p}/\rho$ , Greek indices denote Cartesian coordinates, and the explicit dependence of the CG fields on  $\mathbf{r}$  and  $t$  has been omitted for compactness. Since this paper focuses on the stress field, we have omitted the energy equation, which can be derived in a similar way [27].

In addition to obtaining the standard equations of continuum mechanics from microscopic consideration, this coarse graining procedure provides an expression for the stress tensor  $\sigma_{\alpha\beta}$  in terms of the microscopic entities:

$$\begin{aligned} \sigma_{\alpha\beta}(t) &= -\sum_i m_i v'_{i\alpha}(\mathbf{r}, t) v'_{i\beta}(\mathbf{r}, t) \phi(\mathbf{r} - \mathbf{r}_i(t)) \\ &\quad -\frac{1}{2} \sum_{ij; i \neq j} f_{ij\alpha}(t) r_{ij\beta}(t) \int_0^1 ds \phi[\mathbf{r} - \mathbf{r}_i(t) + s \mathbf{r}_{ij}(t)], \end{aligned} \quad (4)$$

where  $\mathbf{v}'_i(\mathbf{r}, t) \equiv \mathbf{v}_i(t) - \mathbf{v}(\mathbf{r}, t)$  is the fluctuating velocity,  $\mathbf{f}_{ij}(t)$  is the force exerted on particle  $i$  by particle  $j$ , and  $\mathbf{r}_{ij}(t) \equiv \mathbf{r}_i(t) - \mathbf{r}_j(t)$ .

The first term in Eq. (4) is the kinetic stress (which vanishes for static configurations), and the second term is known as the contact stress. Note that the standard Born-Huang expression [55]:  $\sigma_{\alpha\beta} = -\frac{1}{2V} \sum_{ij \in V; i \neq j} f_{ij\alpha} r_{ij\beta}$  is

equivalent to the expression for the contact stress in Eq. (4) if the coarse-graining function is taken constant inside a volume  $V$  and zero outside it, provided that the interparticle separation is much smaller than the coarse-graining length scale (typically  $\sqrt[3]{V}$ ).

The above expressions can be used to calculate the macroscopic fields from the microscopic ones (obtained e.g., from simulations or experiments), and compare them to the predictions of macroscopic models or direct experimental results. In order to close the set of continuum equations [Eqs. (3)] the stress and energy flux (the latter is not related to the considerations below) need to be expressed as functionals of the pertinent *macroscopic* fields. As mentioned, such constitutive relations are often obtained empirically or conjectured. In some cases they are derived from the microscopic dynamics. The above *exact* expression for the stress field provides a framework for a systematic derivation of constitutive relations (as suggested for elastic networks in [27]).

Here, we are concerned with the interpretation of experimental data in terms of microscopic variables and macroscopic fields. The fact that the contact stress includes a sum over all contacts for each particle (i.e., even for very small CG scales the stress components correspond to specific “averages” over the forces on each particle) already suggests that a “picture” of the forces in the packing does not correspond directly to the macroscopic stress field (they are certainly related, i.e., one would usually expect large stress components in regions where large force magnitudes are observed). In particular, as shown in Sec. 2, and further discussed below, force chains do not necessarily indicate macroscopic anisotropy or inhomogeneity.

## 4

### Numerical results for model frictionless systems

Consider a two-dimensional system of uniform disks (arranged on a triangular lattice) subject to a vertical external force at the center of the top layer [26]. Experiments on such systems are described in [22, 23]. Consider first the case of nearest neighbor harmonic interactions, i.e., the disks are coupled by equal linear springs (whose rest length is the diameter of a disk). Clearly, real cohesionless particles do not experience any significant attractive interactions; however, there are a few insights to be obtained from the study of this system. Fig. 5 presents the forces in the system. Force chains are evident.

A contour plot of the “vertical stress component”  $\sigma_{zz}$  [computed using Eq. (4)] for the same system is shown in Fig. 6 (with  $\phi(\mathbf{r}) = \frac{1}{\pi w^2} e^{-(|\mathbf{r}|/w)^2}$ , and  $w = d$ , the particle diameter, i.e., a fine resolution). The force chains are not evident any more. The model described above corresponds, in the continuum (long-wavelength) limit, to an isotropic 2D elastic medium [56]. The observed force chains, which break isotropy, can be attributed to the fact that the local environment of a particle in contact with a finite number of other particles cannot be isotropic. Under homogeneous macroscopic deformation, all forces would be equal in a lattice configuration. However, the concentrated applied force yields an inhomogeneous deformation, which leads to the local anisotropy being reflected

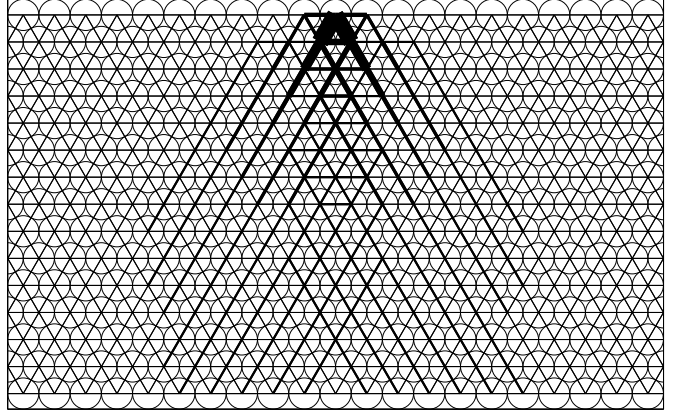


**Fig. 5.** Force chains in a 2D triangular lattice. A vertical force is applied at the center of the top layer. Line widths are proportional to the force magnitudes. Only the central part of the system is shown; reproduced from [26].

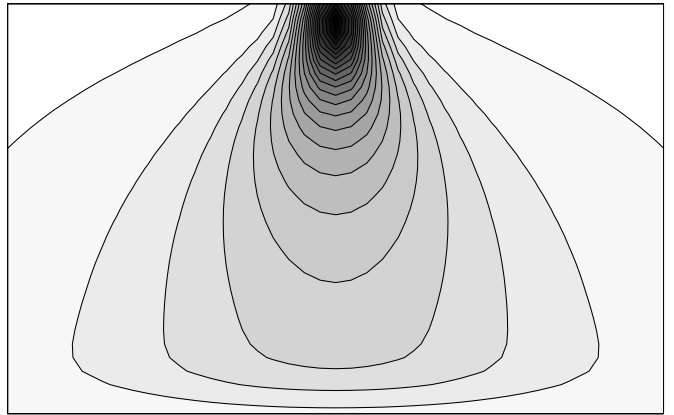


**Fig. 6.** Contour plot of  $h\sigma_{zz}$ , corresponding to Fig. 5 ( $h$  is the slab height); reproduced from [26].

in the distribution of the forces. The elastic continuum description of the stress (to linear order in the strain) is isotropic, and cannot be expected to reflect this microscopic anisotropy. For small system sizes (in which the strain gradients on a particle scale are relatively large), this anisotropy can be observed in the stress field (a very clear example is shown in [26] for a macroscopically isotropic 3D system, whose microscopic symmetry is cubic). These results, as well as those presented in Sec. 1 for disordered elastic systems, show that force chains do not necessarily indicate anisotropy or inhomogeneity of the material on sufficiently large scales; more importantly their existence does not require a non-elastic (microscopic) interaction.

Note that only the forces between the particles and the floor (a single such force per particle) are used in the calculation of the stress at the bottom of the packing. Hence on the bottom (but not in the bulk of the system), the spatial distribution of  $\sigma_{zz}$  is equivalent (up to coarse-graining) to that of the microscopic forces. For sufficiently large systems, the distribution of forces on the bottom corresponds closely to the stress calculated using linear elasticity [26], even “almost without coarse-graining”, i.e., for a microscopic CG scale.

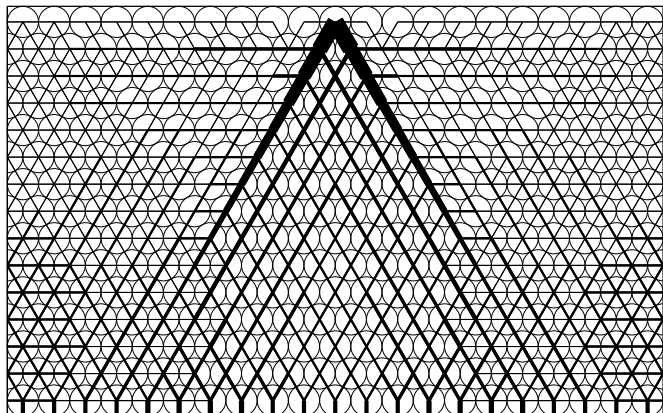


**Fig. 7.** Force chains in a 2D triangular lattice of ‘one-sided’ springs. A gravitational force has been applied in order to stabilize the system (the applied force is 150 times the particle weight); reproduced from [26].

A more realistic force model consists of ‘one-sided’ springs, i.e., springs that snap when in tension. Fig. 7 presents the forces obtained for the same system presented in Fig. 7, but with ‘one-sided’ springs. Compared to the system of regular springs, the application of the concentrated force at the top of the packing leads to rearrangements in the contact network: some horizontal springs in the region under the point where the force is applied are disconnected (as also observed in [57] for a pile geometry) but the force chains in both systems are qualitatively similar. The force distribution vs. the horizontal coordinate at different depths is in good agreement [26] with experiment [22, 23]. For slightly disordered systems [26], the force chains are qualitatively similar, though somewhat shorter.

The corresponding vertical stress field  $\sigma_{zz}$  is shown in Fig. 8. The stress field in this case is clearly quite different from that obtained using ‘two-sided’, harmonic springs: the response for ‘one-sided’ springs is double-peaked. This is obviously related to the disconnected springs below the point of application of the external force. In [26], it has been shown that a model with harmonic springs in which the spring constant for the horizontal springs,  $K_1$ , is different from that of the oblique springs,  $K_2$ , corresponds (in the continuum limit) to an anisotropic elastic system. For sufficiently large  $K_2/K_1$ , the response of such an elastic system has two peaks [26] (see also [18] for a more detailed analysis of the case of an infinite half-plane; the results presented in [26] are for a finite slab on a rigid floor). The absence of horizontal springs corresponds to the limit  $K_2/K_1 \rightarrow \infty$ , the extreme anisotropic limit, which corresponds to an isostatic system. Note that the *stress* field, but not the displacement, depends only on  $K_2/K_1$ . In the case considered here,  $K_1 = 0$  and  $K_2$  is finite; for  $K_2 \rightarrow \infty$ , the rigid limit, the displacement is zero. The double peaked stress distributions are similar to those obtained from hyperbolic models. It follows that hyperbolic-like behavior can be obtained using an *anisotropic* (yet, still elliptic) elastic model (which becomes formally ‘hyperbolic’ in the limit of very large anisotropy; see also [18, 58]).

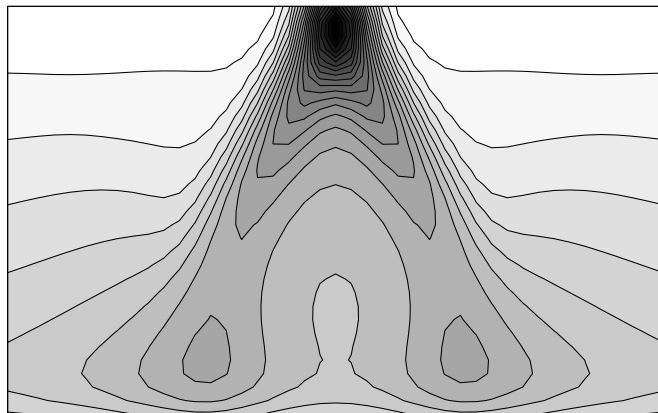


**Fig. 8.** Same as Fig. 6, for the case of ‘one-sided’ springs (for which the forces are shown in Fig. 7); reproduced from [26].

The ‘stress-induced anisotropy’ [26] observed in the case of ‘one-sided’ springs can be thought of as a non-linear extension of the linear elastic continuum behavior obtained in a network of harmonic springs. While the (possibly position-dependent) elastic moduli in linear elasticity are time-independent material properties, a possible extension would be to introduce a stress history dependence of the elastic moduli (i.e., the anisotropy induced by the breaking of contacts in certain regions may be considered a result of a tensile stress in those regions). A similar type of stress-induced anisotropy has been suggested in the context of plastic models for soil mechanics [59]. If the particle positions do not change significantly, so that only the contact network is modified in response to the applied stress, the behavior can possibly be modeled as ‘incrementally elastic’. Under certain condition (corresponding to plastic yield), the system would no longer be able to support the applied stress without a major rearrangement of the particles. Incipient plastic yield may possibly be related to a local extreme anisotropy typical of a marginally stable isostatic configuration.

The force chains obtained both for the harmonic case and the ‘one-sided’ case are quite similar [26] to those observed experimentally [22, 23], as an average over different realizations. This averaging is required due to experimental variations: although the particles are arranged on lattice, there is still some disorder present due to some variability in particle diameter, and possibly also in the contact properties [60]. Indeed, while perfect atomic lattices may be obtained at low enough temperatures, since all atoms of the same isotope are exactly identical, macroscopic particles are never truly identical, so that perfect periodicity can never be obtained. It also appears that the force chains obtained using the two models are quite similar (similar chains are also obtained in slightly disordered systems [26]). The stress field appears to be more sensitive to the anisotropy induced by the applied force.

In the experiments reported in [20, 21, 24], the forces on the floor were measured. In [20, 21], the width of the pressure probe (which would correspond to the CG scale of the measured stress) was 10 – 30 particle diameters. The bottom stress profiles measured are quite consistent with continuum elasticity (note that the depths of the

systems studied were 20 – 300 particle diameters). Experimental deviations from the predictions of *isotropic* elasticity [21] can be reproduced by anisotropic elasticity [26]. Narrower or wider peaks than those obtained for isotropic systems can be obtained for small anisotropy, while for very large anisotropy, two peaks are expected (see also [18]). An additional possible cause for deviations from the isotropic elastic calculations presented in [21] is finite rigidity of the floor [56]. The more shallow systems used in the experiments may even be small enough for the finite size effects [26] to be significant. Any anisotropy in these experiments is obviously much weaker than the strong anisotropy observed in the model ordered system of ‘one-sided’ springs. Several effects may explain this: first, the systems used in the experiment are highly disordered, so that inhomogeneous, random anisotropy may be expected on intermediate (already macroscopic) scales, presumably averaging out to an isotropic, or nearly isotropic, behavior at sufficiently large scales. In this case, the large-scale effect of contacts breaking due to applied forces would be significantly less pronounced than in the ordered system described above. A second possibility is the effect of frictional forces, which may either prevent contacts from breaking, or reduce the anisotropy of the response. Third, the model systems discussed above were unstressed before the application of the force, while the experimental ones are pre-stressed by gravity, which may compress some of the contacts such that the tension due to the applied force is insufficient to break them.

In [24], individual forces on the floor were measured, and the results were averaged over realizations (which, as mentioned, is not necessarily equivalent to spatial coarse-graining). The regular packings used in [24] (FCC and HCP) are macroscopically anisotropic. The fact that some of the horizontal contacts (contacts among particles in the same layer) may be absent increases the anisotropy further (possibly in an inhomogeneous way; as mentioned above, a granular packing cannot be perfectly periodic). The extreme limit in which there are no such horizontal contacts corresponds to an isostatic system. Such anisotropy (possibly further enhanced by the applied force) may explain the discrete peaks observed for relatively shallow systems composed of 9 layers of particles (and the fact that they appear to be consistent with a picture of “force propagation” appropriate for isostatic systems). However, for deeper system (about 20 particle diameters), there appears to be a crossover to a smoother behavior, which should correspond to the crossover to the continuum limit (note that the depth of the systems used in [24] was smaller than the depth required in our calculations on 3D systems [26] for reaching the continuum limit, so deeper systems may still show dependence on the depth).

## 5 Effects of Friction

As shown, some features of granular response may be reproduced using models employing frictionless and even harmonically interacting particles. However, it is clear that friction is consequential for granular materials.

For frictional spheres, the microscopic description, as described in Sec. 2, must be extended to include (at least) the orientations of the particles, and interparticle torques in addition to the forces. The description of static and kinetic friction requires the use of more complicated force models, which depend on the particle orientations and their relative tangential velocities, and possibly on the history of contact deformation (see e.g., [37–39, 61]).

In experiments performed on regular 2D packings of photoelastic disks [23], the directions and “strengths” of the force chains observed upon application of a localized force to the top of the packing appear to depend quite strongly on the angle of the applied force with respect to the horizontal (in the following, all angles are given with respect to the horizontal). A particularly intriguing effect is that for some angles, force chains appear not only in the lattice directions ( $0, \pm 60^\circ, \pm 120^\circ, 180^\circ$  for a triangular lattice), but also, apparently, in new directions which can be identified as  $\pm 30^\circ$  (in fact, in individual realizations, rather than their average as reported in [23], it appears that force chains appear also at  $\pm 90^\circ$ , i.e., the vertical direction [60]). These directions correspond to next-nearest neighbor directions in the triangular lattice. Since interactions among the particles only exist for particles in contact, there is no direct next-nearest neighbor interaction. The fact that the forces themselves, and not just the contact points, appear to be aligned with these  $\pm 30^\circ$  directions, suggests that frictional forces among the particles (tangential to the contact normals, which result in interparticle torques) are necessary for obtaining forces (and chains) at angles different from the lattice directions. For an applied force at  $\pm 90^\circ$ , it appears that the frictional forces are small enough such that the results obtained in this case [22, 23] are described quite well by a model of frictionless particles with linear force-displacement laws [26].

In order to elucidate the role of frictional forces and torques in the quasi-static response of granular materials in general, and in particular in order to gain an understanding of the experimental results mentioned above [23], we performed discrete element simulations with normal and tangential linear spring-dashpot forces among the particles (see e.g., [10, 32]), possibly the simplest model for frictional disks. The simulation parameters were chosen to correspond to those of the experimental system [60]. Experimentally, the force-displacement law for the photoelastic disks was found to be fit quite well by  $f \propto \xi^{3/2}$  [60], as predicted by the standard Hertz theory for elastic ellipsoids in contact (see e.g. [36]), rather than the linear relation (with logarithmic correction) expected for cylinders in contact [62], which appears to imply that the contact region between the “disks” is elliptic rather than rectangular. The simulation model described above employs a linear force-displacement law, so that an effective mean spring constant was estimated on the basis of the range of forces used in the experiments. The tangential spring constant was taken to be one-half the normal spring constant (a rough estimate consistent with the Hertz-Mindlin model [63] for oblique contact forces). The normal and tangential spring constants used are  $k_n = 3000\bar{m}g/\bar{R}$  and  $k_t = 1500\bar{m}g/\bar{R}$ , where  $\bar{R}$  and  $\bar{m}$  are the mean particle radius and mass, respectively, and  $g$  is the gravitational



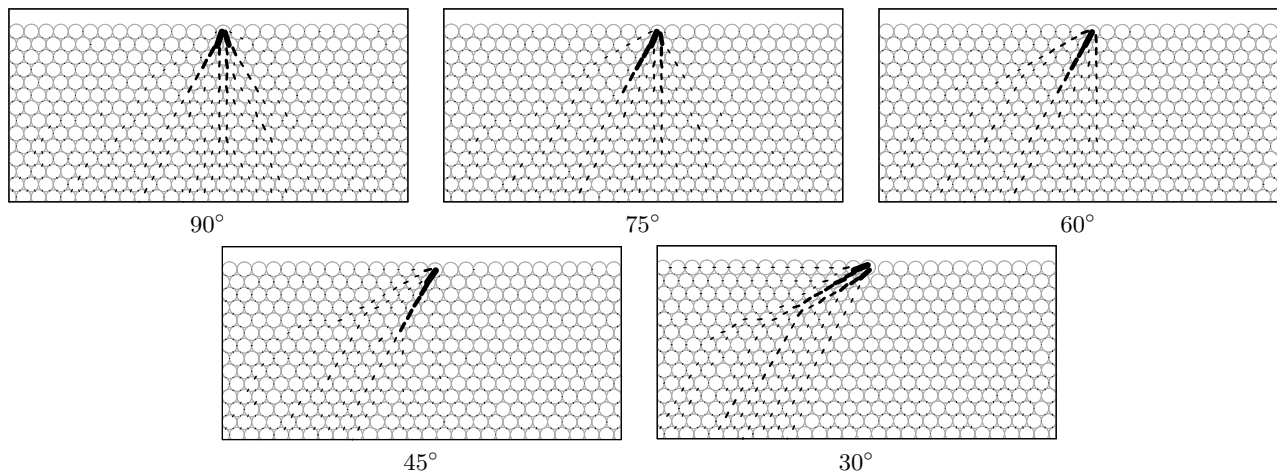


**Fig. 9.** Force chains in 2D packings of slightly polydisperse frictional particles. A force  $F$  with magnitude 150 times the mean particle weight is applied to the particle at the center of the top layer. The angle of the force with respect to the horizontal is indicated below each picture. The same realization of the packing was used in all cases. The region shown is the central third of the upper half of the system.

acceleration. The friction coefficient used is  $\mu = 0.94$  for particle-particle contacts and  $\mu^{\text{wall}} = 0.35$  for particle-wall contacts. The systems studied here are composed of polydisperse disks, with radii distributed uniformly in the interval  $[R - \delta R, R]$ , where  $\delta R/R = 8 \cdot 10^{-3}$  (i.e., a small polydispersity).

The system is first relaxed to a static state under gravity (until the total kinetic energy per particle is less than  $10^{-9} \bar{m} g \bar{R}$ ), and then relaxed again with an external force applied at the center of the top layer (in some cases the force was increased linearly with time from zero to prevent the “buckling” of the top layer which leads to major rearrangements; these are beyond the nearly elastic behavior considered here).

For comparison with the experiments presented in [23], an external force of magnitude  $F = 150 \bar{m} g$  was applied to the center top particle at angles of  $15^\circ$ ,  $30^\circ$ ,  $45^\circ$ ,  $60^\circ$ ,  $75^\circ$ , and  $90^\circ$ . The simulated systems consisted of 29 rows of 80 particles, which is similar to the size of the systems used in the experiments [22, 23, 60]. Fig. 9 presents the forces obtained for different applied force angles. The same particle configuration was used in all cases. No significant particle rotation occurred except for the particles adjacent to the one on which the force is applied. For a force at an angle of  $15^\circ$ , buckling occurred in the top row, causing major rearrangements. Such buckling was also observed in the experiments, where it was apparently stabilized, limiting the rearrangements to a small region near the point of application of the force, but we have not been able to prevent major rearrangements in the simulation. As mentioned, tangential forces such as friction give rise to interparticle torques. Simulations with an applied torque (in addition to the applied force) show that this torque does influence the observed force chains [64].

The results are quite similar, qualitatively, to those observed in the experiment [23]. Note that the results shown in Fig. 9 are for a single configuration, while the results presented in [23] are for an average over configurations. The results obtained in simulations for different realiza-

tions of the disorder are qualitatively similar [64]. The agreement of the results obtained using a relatively simple force model with the experiments is encouraging. A more detailed study of the effects of friction on the forces and the stress field will be presented elsewhere [64].

## 6 Concluding remarks

We have shown that the seemingly inconsistent results of different kinds of experiments studying the static response of granular packings to a concentrated force can all be understood within the same framework of an essentially elastic (elliptic) picture once the distinction between forces and stress is made and the possible consequences of small system size, as well as anisotropy, are taken into account. The effect of applied stresses on the contact network may be modeled as a nonlinear, incrementally elastic model (which may be further extended to describe yielding).

Somewhat surprisingly, many aspects of the response of such systems can be understood using models of frictionless particles. However, some effects do require the introduction of friction, as in the example of the force chains obtained for oblique applied forces described in this paper. We note, however, that the model for the friction used in the simulations described in Sec. 5 consists of tangential springs (with the additional Coulomb condition). This indicates that even for static frictional systems (below yield) an elastic continuum model, which probably includes rotational degrees of freedom (e.g., a Cosserat continuum model [65]), may be appropriate.

Another important issue which requires further study is the effect of disorder, and the relation of spatial averaging to averaging over the disorder.

## References

1. A. Levy and H. Kalman, editors, *Handbook of Conveying and Handling of Particulate Solids*, Elsevier, 2001.

2. H. M. Jaeger, S. R. Nagel, and R. P. Behringer, *Physics Today* **49**, 32 (1996).
3. H. M. Jaeger, S. R. Nagel, and R. P. Behringer, *Rev. Mod. Phys.* **68**, 1259 (1996).
4. P. G. de Gennes, *Rev. Mod. Phys.* **71**, S374 (1999).
5. L. P. Kadanoff, *Rev. Mod. Phys.* **71**, 435 (1999).
6. I. Goldhirsch, *Ann. Rev. Fluid Mech.* **35**, 267 (2003).
7. R. M. Nedderman, *Statics and Kinematics of Granular Materials* (Cambridge University Press, 1992).
8. S. B. Savage, Modeling and granular materials boundary value problems, in *Proceedings of the NATO Advanced Study Institute on Physics of Dry Granular Media, Cargèse, France, September 15-26, 1997*, edited by H. J. Herrmann, J. P. Hovi, and S. Luding, pp. 25–95, Kluwer, 1998.
9. A. Drescher and G. de Josselin de Jong, *J. Mech. Phys. Solids* **20**, 337 (1972).
10. P. A. Cundall and O. D. L. Strack, *Geotechnique* **29**, 47 (1979).
11. F. Radjai, S. Roux, and J. J. Moreau, *Chaos* **9**, 544 (1999).
12. J. P. Wittmer, P. Claudin, M. E. Cates, and J.-P. Bouchaud, *Nature* **382**, 336 (1996).
13. J.-P. Bouchaud, M. E. Cates, and P. Claudin, *J. de Physique I* **5**, 639 (1995).
14. J. P. Wittmer, M. E. Cates, and P. Claudin, *J. de Physique I* **7**, 39 (1997).
15. A. V. Tkachenko and T. A. Witten, *Phys. Rev. E* **60**, 687 (1999).
16. J.-P. Bouchaud, P. Claudin, D. Levine, and M. Otto, *Eur. Phys. J. E* **4**, 451 (2001).
17. J. E. S. Socolar, D. G. Schaeffer, and P. Claudin, *Eur. Phys. J. E* **7**, 353 (2002).
18. M. Otto, J.-P. Bouchaud, P. Claudin, and J. E. S. Socolar, *Phys. Rev. E* **67**, 031302 (2003).
19. M. D. Silva and J. Rajchenbach, *Nature* **406**, 708 (2000).
20. G. Reydellet and E. Clément, *Phys. Rev. Lett.* **86**, 3308 (2001).
21. D. Serero, G. Reydellet, P. Claudin, E. Clément, and D. Levine, *Eur. Phys. J. E* **6**, 169 (2001).
22. J. Geng *et al.*, *Phys. Rev. Lett.* **87**, 035506 (2001).
23. J. Geng, G. Reydellet, E. Clément, and R. P. Behringer, *Physica D* **182**, 274 (2003).
24. N. W. Mueggenburg, H. M. Jaeger, and S. R. Nagel, *Phys. Rev. E* **66**, 031304 (2002).
25. C. F. Moukarzel, H. Pancheco-Martínez, J. C. Ruiz-Suarez, and A. M. Vidales, cond-mat/0308240.
26. C. Goldenberg and I. Goldhirsch, *Phys. Rev. Lett.* **89**, 084302 (2002).
27. I. Goldhirsch and C. Goldenberg, *Eur. Phys. J. E* **9**, 245 (2002).
28. A. Tanguy, J. P. Wittmer, F. Leonforte, and J.-L. Barrat, *Phys. Rev. B* **66**, 174205 (2002).
29. C. F. Moukarzel, *Granular Matter* **3**, 41 (2001).
30. D. A. Head, A. V. Tkachenko, and T. A. Witten, *Eur. Phys. J. E* **6**, 99 (2001).
31. L. E. Silbert, D. Ertas, G. S. Grest, T. C. Halsey, and D. Levine, *Phys. Rev. E* **65**, 031304 (2001).
32. H. J. Herrmann and S. Luding, *Cont. Mech. and Thermodynamics* **10**, 189 (1998).
33. D. E. Wolf, Modeling and computer simulation of granular media, in *Computational Physics*, edited by K. H. Hoffmann and M. Schreiber, pp. 64–94, Springer, Heidelberg, 1996.
34. G. M. L. Gladwell, *Contact Problems in the Classical Theory of Elasticity* (Sijthoff & Noordhoff, The Netherlands, 1980).
35. K. L. Johnson, *Contact Mechanics* (Cambridge University Press, Cambridge, 1985).
36. L. Landau and E. Lifshitz, *Theory of Elasticity, 3rd Edition* (Pergamon, 1986).
37. J. Schäfer, S. Dippel, and D. E. Wolf, *J. de Physique I* **6**, 5 (1996).
38. M. H. Sadd, Q. Tai, and A. Shukla, *Int. J. of Non-Linear Mech.* **28**, 251 (1993).
39. O. R. Walton, Force models for particle-dynamics simulations of granular materials, in *Mobile Particulate Systems*, edited by E. Guazzelli and L. Oger, pp. 367–380, Kluwer, 1995.
40. C. F. Moukarzel, *Phys. Rev. Lett.* **81**, 1634 (1998).
41. J.-N. Roux, *Physical Review E* **61**, 6802 (2000).
42. H. Makse, D. L. Johnson, and L. M. Schwartz, *Phys. Rev. Lett.* **84**, 4160 (2000).
43. D. W. Howell and R. P. Behringer, *Chaos* **9**, 559 (1999).
44. D. M. Mueth, H. M. Jaeger, and S. R. Nagel, *Phys. Rev. E* **57**, 3164 (1998).
45. D. L. Blair, N. W. Mueggenburg, A. H. Marshall, H. M. Jaeger, and S. R. Nagel, *Phys. Rev. E* **63**, 041304 (2001).
46. F. Radjai, M. Jean, J.-J. Moreau, and S. Roux, *Phys. Rev. Lett.* **77**, 274 (1996).
47. J. M. Erikson, N. W. Mueggenburg, H. M. Jaeger, and S. R. Nagel, *Phys. Rev. E* **66**, 040301 (2002).
48. M. L. Nguyen and S. N. Coppersmith, *Phys. Rev. E* **62**, 5248 (2000).
49. L. E. Silbert, G. S. Grest, and J. W. Landry, *Phys. Rev. E* **66**, 061303 (2002).
50. C. S. O'Hern, S. A. Langer, A. J. Liu, and S. R. Nagel, *Phys. Rev. Lett.* **86**, 111 (2000).
51. C.-H. Liu *et al.*, *Science* **269**, 513 (1995).
52. S. N. Coppersmith, C.-H. Liu, S. Majumdar, O. Narayan, and T. A. Witten, *Phys. Rev. E* **53**, 4673 (1996).
53. C. S. O'Hern, S. A. Langer, A. J. Liu, and S. R. Nagel, *Phys. Rev. Lett.* **88**, 075507 (2002).
54. B. J. Glasser and I. Goldhirsch, *Phys. Fluids* **13**, 407 (2001).
55. M. Born and K. Huang, *Dynamical theory of crystal lattices* (Clarendon Press, Oxford, 1988).
56. C. Goldenberg and I. Goldhirsch, Unpublished.
57. S. Luding, *Phys. Rev. E* **55**, 4720 (1997).
58. M. E. Cates, J. P. Wittmer, J.-P. Bouchaud, and P. Claudin, *Chaos* **9**, 511 (1999).
59. M. Oda, *Mech. Mat.* **16**, 35 (1993).
60. J. Geng and R. P. Behringer, private communication (2002).
61. L. Vu-Quoc and X. Zhang, *Mech. Mat.* **31**, 235 (1999).
62. J. Schwartz and E. Y. Harper, *Int. J. Solids and Structures* **7**, 1613 (1971).
63. R. D. Mindlin and H. Deresiewicz, *J. Appl. Mech.* **20**, 327 (1953).
64. C. Goldenberg and I. Goldhirsch, In preparation.
65. A. C. Eringen, Theory of micropolar elasticity, in *Fracture: An Advanced Treatise, Volume II: Mathematical Fundamentals*, edited by H. Liebowitz, pp. 621–729, Academic Press, New York and London, 1968.